1 **Original Article：**

2

3 **Title: Phosphate glass fibers facilitate proliferation and osteogenesis through**

4 **Runx2 transcription in murine osteoblastic cells**

5

6 **Authors:** Xiao Lin[1,2,3,#], Qiang Chen[4,#]，Yunyun Xiao[1,2,3], Yongguang Gao[1,2,3], Ifty Ahmed[5],

7 Meng Li[6], Hui Li[7], Kewen Zhang[1,2,3], Wuxia Qiu[1,2,3], Xianhu Liu[8], Aldo R. Boccaccini[9], Airong

8 Qian[1,2,3,*]

9

10 Affiliations:

11 1. Lab for Bone Metabolism, Key Lab for Space Biosciences and Biotechnology, School of Life

12 Sciences, Northwestern Polytechnical University, Xi'an, Shaanxi 710072, China

13 2. Research Center for Special Medicine and Health Systems Engineering, School of Life

14 Sciences, Northwestern Polytechnical University, Xi'an, Shaanxi 710072, China

15 3. NPU-UAB Joint Laboratory for Bone Metabolism, School of Life Sciences, Northwestern

16 Polytechnical University, Xi'an, Shaanxi 710072, China

17 4. State Key Laboratory of Solidification Processing, Northwestern Polytechnical University,

18 Xi'an, Shaanxi 710072, China

19 5. Faculty of Engineering, Advanced Materials Research Group, University of Nottingham,

20 Nottingham NG 7 2RD, United Kingdom

21 6. School of Life Sciences, Northwestern Polytechnical University, Xi'an, Shaanxi 710072, China

22 7. Honghui hospital, Xi'an Jiaotong University, Xi'an, Shaanxi 710072, China

23 8. National Engineering Research Center for Advanced Polymer Processing Technology,

24 Zhengzhou University, Zhengzhou, 450002, China

25 9. Institute of Biomaterials, University of Erlangen-Nuremberg, Cauerstrasse 6, 91058 Erlangen,

26 Germany

27 #：The authors are equal to this work.

28 * Corresponding author: Prof. Airong Qian

29 School of Life Sciences, Northwestern Polytechnical University, Xi'an, Shaanxi 710072, China

30 Tel: +86-029-8849-1840, E-mail address: qianair@nwpu.edu.cn

ABSTRACT

Cell-material interactions and compatibility are important aspects of bioactive materials for bone tissue engineering. Phosphate glass fiber (PGF) is an attractive inorganic filler with fibrous structure and tunable composition, which has been widely investigated as a bioactive filler for bone repair applications. However, the interaction of osteoblasts with PGFs has not been widely investigated to elucidate the osteogenic mechanism of PGFs. In this study, different concentrations of short PGFs with interlaced oriented topography were co-cultured with MC3T3-E1 cells for different periods, and the synergistic effects of fiber topography and ionic product of PGFs on osteoblast responses including cell adhesion, spreading, proliferation and osteogenic differentiation were investigated. It was found that osteoblasts were more prone to adhere on PGFs through vinculin protein, leading to enhanced cell proliferation with polygonal cell shape and spreading cellular actin filaments. In addition, osteoblasts incubated on PGF meshes showed enhanced alkaline phosphatase (ALP) activity, extracellular matrix mineralization, and increased expression of osteogenesis-related marker genes, which could be attributed to the Wnt/β-catenin/Runx2 signaling pathway. This study elucidated the possible mechanism of PGF on triggering specific osteoblast behavior, which would be highly beneficial for designing PGF-based bone graft substitutes with excellent osteogenic functions.

Keywords: Cell-material interaction, Phosphate glass fibers, Osteogenesis, Signaling pathway, Runx2;

1. Introduction

Bone loss is one of the most important causes of skeletal disease such as congenital defects, oral and maxillofacial pathologies and osteoporosis leading to bone fractures[1]. Many studies focus on bone tissue engineering strategies for skeletal tissue regeneration. In bone tissue engineering, engineered scaffolds can provide specific microenvironment and architecture for cell adhesion, migration, proliferation and even bone formation by regulating osteogenic differentiation[2]. The stiffness, elasticity, topography, morphology and specific degradation products of the scaffold can regulate cell-cell, cell-ECM and cell-material interactions[3]. Scaffold architecture is reported to be critically important for bone regeneration as it could be made to mimic the native 3D environment for osteoblasts in order to promote cell adhesion and activation[4, 5]. In addition, bioactive constituents of the scaffold are also important characteristics of bone tissue engineering materials[6]. On the one hand, materials can provide bioactivity to interact with surrounding cells and tissues and avoid the host immune response[7]. On the other hand, biomaterial surfaces can present osteo-inductive factors such as calcium ions and growth factors to the local microenvironment in order to enhance bone formation[7, 8].

Phosphate-based glasses have gained increasing attention[9, 10], because of their similar composition to the inorganic component of native bone, biocompatibility, bioactivity, and osteo-conductivity[11, 12]. It has been previously reported that biodegradable composites reinforced with phosphate glass fibers (PGFs) could promote the proliferation of preosteoblasts[13]. PGFs have also been shown to promote neuronal polarization and directional growth of axons *in vitro* and *in vivo*, potentially repairing peripheral nerve injury *in vivo*[14-16]. In addition, fibrous chitosan-glued phosphate glass fiber scaffolds were shown to be non-cytotoxic against bone marrow stromal cells[17]. Furthermore, nanocomposite polymer scaffolds using sacrificial phosphate glass fibers have shown support for the growth of human tenocytes cells[18]. It was also recently reported that PGFs can be deposited as coating on bulk metallic surfaces to enhance the proliferation and expression of osteogenic-related genes in MC3T3-E1 cells[19]. These attractive characteristics and higher bioactivity of PGFs suggest that they can be considered suitable building blocks for bone scaffolds and can function as an excellent tissue engineering material.

Osteogenic differentiation involves several key steps including cellular proliferation, extracellular matrix (ECM) synthesis, and ECM mineralization[20]. The corresponding signaling

1   systems related to osteogenesis and bone growth include Wnt signal pathway, transforming

2   growth factor beta (TGF-β) signal pathway, mitogen-activated protein kinases (MAPK) signal

3   pathway among others[21]. Transcription factors play an important role in regulating proliferation

4   and differentiation of osteoblasts[20]. Runt-related transcriptional factor 2 (Runx2), an

5   osteoblast-specific transcription factor, can combine with osteoblast specific cis element in the

6   osteocalcin promoter[22] and regulate the process of mesenchymal stem cell differentiation into

7   osteoblasts by promoting the expression of osteoblast-specific genes, such as ALP, OCN, and

8   ColI[23]. Studies have reported that overexpression of Runx2 could induce osteogenesis *in vitro* and

9   *in vivo*, and also accelerate the healing of bone defects in the skulls of mice[24].

10   It has been reported that calcium ion induced Wnt signalling is essential for bone tissue

11   formation[25-27]. Wnt/β-catenin is an important upstream signal transduction of Runx2 for regulating

12   bone formation and bone metabolism diseases by influencing the expression of osteogenic specific

13   genes[28]. During osteogenesis, Wnt signaling is activated, non-phosphorylated β-catenin in

14   cytoplasm accumulates and translocates into the nucleus and then β-catenin binds with

15   Groucho/TCF/LEF complex to induce gene transcription[29]. Inhibition of Wnt/β-catenin activation

16   was found to reduce bone formation in mice[30].

17   Many studies have indicated that PGFs with their fibrous structure and tunable composition

18   offer great potential for biomedical applications. Previous work by some of the authors reported

19   that P50 PGFs was sufficient for muscle cell attachment and differentiation[12]. However, the

20   interaction of osteoblasts with P50 PGFs and the mechanism of P50 PGFs on the function of

21   osteoblasts are not fully understood. In this study, P50 PGFs were employed to investigate the

22   influence of topography and degradation products on osteoblasts behavior, including cell

23   spreading, adhesion, proliferation and differentiation. Moreover, the mechanism of PGFs on

24   osteogenic marker expression and osteogenesis ability has also been investigated to generate new

25   insights into the osteoblast-PGF interaction. The underlying mechanisms established will provide

26   useful hints for further bone tissue regeneration and PGF-based medical device development

27   strategies.

28   **2. Materials and Methods**

29   **2.1 Materials fabrication**

30   Phosphate glass fibers were produced using NaH_2PO_4, $CaHPO_4$, $FePO_4 \cdot 2H_2O$, and P_2O_5 as

1　raw materials (Sigma Aldrich, UK), as reported previously by Felfel et al[31]. Briefly, The

2　precursors were weighed according to the nominal composition $50P_2O_5–40CaO_5–5Na_2O–5Fe_2O_3$

3　(in mol%) ——denoted as P50, and then melted in a Pt-Au crucible at 1100 ℃ for 90 min.

4　Continuous fibers with a diameter in the range ~10-20 μm were then produced from the molten

5　glass via an in-house melt-draw spinning facility at ~1600 rpm, followed by annealing at 5 ℃

6　below the glass transition temperature (Tg=479℃) for 90 min. The as-prepared PGF bundles were

7　chopped into short PGF meshes with the length of 2-3 mm before further utilization.

8　**2.2 Morphology and calcium ion release measurements**

9　Chopped PGFs were immersed in 75 vol% ethanol, subjected to ultrasonication treatment for

10　20 min, and then dried in vacuum desiccator at 50℃ overnight. The samples were adhered onto a

11　sample holder using conductive carbon tape and then sputter-coated with gold for 1.5 min.

12　Scanning electron microscopy (SEM, TESCAN VEGA 3 SBH) and energy dispersive X-ray

13　Spectrometer (EDX, Bruker Instruments, Germany) were used to evaluate the morphology and

14　elemental composition of the produced PGFs. For calcium ion release test, 0.05 g of PGFs were

15　added in a plastic bottle containing 30 ml PBS and placed inside an incubator at 37℃. After 3 h, 6

16　h, 12 h, 24 h, 3 d, 7 d, 14 d and 21 d, 3 ml of the supernatant was extracted for measurement, and

17　the bottle was refilled with another 3 ml of fresh PBS to maintain constant volume of release

18　medium. The calcium concentration was measured by atomic absorption spectroscopy (ZEEnit

19　700P, Analytik Jena AG, Germany). Three replicates were measured at each time point.

20　**2.3 Cell culture**

21　MC3T3-E1 cell line was purchased from ATCC (Manassas, USA) and cultured in α-MEM

22　(Gibco, Carlsbad, USA) supplemented with 10% FBS (Biological Industries, Kibbutz

23　BeitHaemek, Israel), 1% L-glutamine (Sigma–Aldrich, St. Louis, MO), 100 U/ml penicillin and

24　100 μg/ml streptomycin. Osteogenesis of MC3T3-E1 cells was induced by condition medium in

25　α-MEM (Gibco, Carlsbad, USA) supplemented with 10% FBS (Gibco, Carlsbad, USA), 100

26　μg/ml streptomycin, 100 U/ml penicillin, 50 μg/ml ascorbicacid and 10 mM β–glycerophosphate

27　(Sigma-Aldrich, MO, USA). The density of cells to be seeded was 6×10^5 cells per well of

28　24-well plate. Cells were incubated at 37℃ using a 5% CO_2 incubator.

29　**2.4 Cell proliferation**

30　For cell proliferation assay, MC3T3-E1 cells were seeded with different concentrations of

PGFs (0, 0.5 and 1 mg/ml) in 24-well plate. After culturing in condition medium for 0 d, 3 d and 5

d respectively, the proliferation ability of the cells was analyzed by Cell Counting Kit-8 (CCK-8)

(Beyotime Institution of Biotechnology, Jiangsu, China). Briefly, 300 μl of CCK-8 regent was

added in each well and incubated for another 2 h at 37℃. And then absorbance was detected at

450 nm using microplate reader (Synergy HT, BioTek, USA). The results were expressed as the

mean absorbance of four parallel tests.

2.5 Immunofluorescence assay

MC3T3-E1 cells were seeded with different concentrations of PGFs (0, 0.5 and 1 mg/ml).

After the predetermined time point in condition medium, cells were washed 2-3 times with

pre-cooled PBS, then the cells with materials were fixed with 4% paraformaldehyde for 15 min

and washed again with pre-cooled PBS for 2-3 times. The cells were then permeabilized with

0.5% Triton X-100 for 10 min and then washed again 2-3 times with pre-cooled PBS. After which

the cells were then stained with 0.5 μg/ml Phalloidin-TRITC (sigma, USA), 4 μg/ml Vinculin and

2 μg/ml Runx2 in dark overnight respectively. After incubation, cells were washed twice with

pre-cooled   PBS.   Finally,   the   nuclei   were   stained   with   1   μg/ml   of   DAPI

(4,6-diamidino-2-phenylindole) in dark for 3 min, washed twice with pre-cooled PBS for 3-5 min.

The protein expression was observed under fluorescence microscope (Nikon 80i, Japan).

2.6 Alkaline phosphatase (ALP) activity assay

Cells were cultured with different concentrations of PGFs (0, 0.5 and 1 mg/ml) in 24-well

plate with condition medium for 3, 7, 14 and 21 d, respectively. The ALP activity was analyzed by

Alkaline Phosphatase Assay Kit (Beyotime Institution of Biotechnology, Jiangsu, China). Briefly,

the samples were washed with PBS for 2-3 times and then lysed with 50 μl of 0.1% Triton X-100

(Sigma-Aldrich, MO, USA) for 30 min at 4℃. The lysate was centrifuged at 12000 rpm for 10

min at 4℃. 20 μl of supernatant was added into chromogenic substrate and incubated for 10 min

at 37℃. Then the reaction was discontinued by adding stop solution. Absorbance was detected at

405 nm using microplate reader (Synergy HT, BioTek, USA). The results were expressed as the

mean absorbance of three parallel tests.

2.7 Alizarin red S staining

Cells were cultured with different concentrations of PGFs (0, 0.5 and 1 mg/ml) in condition

medium for 0, 3, 7, 14 and 21 d, respectively. Treated cells were fixed in 4% paraformaldehyde

1   for 10 min, and then washed with PBS for 2-3 times. Mineralized nodules were stained by

2   incubating with 0.5% alizarin red (pH=4.2) (Sigma-Aldrich, MO, USA) for 15 min at room

3   temperature. Then the excess stain was washed with double distilled water. The optical images of

4   the stained nodules were observed by scanner (Cannon, Japan).

5   **2.8 Real-Time RT-PCR**

6   MC3T3-E1 cells cultured with different concentrations of PGFs (0, 0.5 and 1 mg/ml) in

7   24-well plate for 3, 7, 14 and 21 d, respectively, and the expression of osteogenic marker genes

8   and adhesion-related genes were detected by Real-time PCR method. Total RNAs were isolated

9   from MC3T3-E1 cells by TRIzol reagent (Invitrogen, USA) according to the manufacturer's

10   instructions, and cDNA was synthesized using one-step PrimeScript RT reagent kit (TaKaRa,

11   Dalian, China) for mRNA analysis. Real-Time PCR assay for mRNA analysis was performed by

12   SYBR Premix Ex TaqIIkit (TaKaRa, Dalian, China). Real-Time RT-PCR was performed using

13   Thermal Cycler C-1000 Touch system (Bio-Rad, Hercules, CA) and GAPDH was used as control

14   for mRNA detection (n=3). Primers used for Real-Time PCR were listed in Table 1.

15   **2.9 Statistical analysis**

16   Data were expressed as mean±SD from independent experiments. *Student's* two-tailed *t*-test

17   was performed to determine the significance of differences. Values were considered statistically

18   significant at **$p<0.01$ or *$p<0.05$.

19   **3. Results**

20   **3.1 Material characterization**

21   The morphology and elemental composition of the synthesized PGFs are showed in Figure 1.

22   The SEM result showed that PGFs possessed smooth surface with a diameter of 12.48 ± 0.19 μm

23   (Figure 1A). Surface EDX analysis was also performed to measure the elemental composition of

24   the produced PGFs. The EDX pattern of the selected area in Figure 1B revealed the presence of

25   calcium, phosphorus, iron, sodium and oxygen, and the atomic composition of the detected

26   elements as presented in the inset table is in agreement with the designed composition (P50). The

27   release profiles of calcium ions from PGFs, which is closely associated with the formation of HA

28   phase, are plotted in Figure 1C. A burst ion release up to 2.69 μg/mg was detected during the first

29   day of incubation, then stable ion release with an additional release amount of 4.34 μg/mg was

30   measured during the whole incubation period.

3.2 Spreading of osteoblasts with PGFs

The morphology of osteoblasts on different concentrations (0, 0.5 and 1 mg/ml) of PGFs in condition medium for 0, 3 and 5 days is shown in Figure 2A. Cells on culture plate with 0 mg/ml of PGFs were used as the control group. Compared with the control group, MC3T3-E1 cells spread well on PGFs. At the beginning of induction, MC3T3-E1 cells cultured without PGFs exhibited completely confluence. However, MC3T3-E1 cells were more inclined to spread towards PGFs with increasing concentrations. After culturing for 5 d, an increasing number of MC3T3-E1 cells was observed on and between the 1 mg/ml of PGF fibers (as indicated by the arrows in Figure 2A).

The cytoskeleton of MC3T3-E1 cells on PGF fibers was performed by labeling the organization of F-actin stress fiber using immunofluorescence assay. The results showed that MC3T3-E1 cells on PGFs possessed wide spreading cellular actin filaments and polygonal cell shape, especially in the 1 mg/ml of PGF group (indicated by the arrows). Whilst the orientated cellular actin filaments and fibroblast-like osteoblasts were seen in the control group (Figure 2B). These results indicated that MC3T3-E1 cells preferred to spread on the PGF fibers with polygonal cell shape, probably due to the interlaced morphology of the PGF meshes and preferential adhesion of osteoblasts on the PGFs.

3.3 Adhesion and proliferation of osteoblasts

MC3T3-E1 cells were seeded on PGFs and cultured in condition medium for 72 h. The adhesion of cells was investigated by double fluorescent labeling of vinculin protein, one of the focal adhesion complexes. Compared with the control group, cells were more prone to adhere onto the surface of the PGFs probably through vinculin (Figure 3A) (as indicated by the arrows). The mRNA expression level of adhesion-related genes including Vinculin, Fibronectin 1 and Collagen type Ⅲ alpha 1 (Col3α1) were selected for the RT-PCR study. The result showed that PGFs increased the expression of Vinculin and Fibronectin 1 significantly (Figure 3B). Therefore, it was concluded that PGFs induced adhesion of osteoblasts in the early osteogenesis stage. The proliferation of MC3T3-E1 cells cultured with the different concentrations of PGFs was assessed using CCK-8 assay. The result showed that 0.5 mg/ml and 1 mg/ml of PGFs significantly promoted the proliferation of MC3T3-E1 cells at day 3 and day 5 (Figure 3C). Hence, it is also suggested that the addition of PGFs, especially for the 1 mg/ml dose, played an important role in

1   the proliferation of MC3T3-E1 cells at the initial stages of osteogenesis.

2   **3.4 ALP activity and Alizarin red S staining of mineralized nodules**

3   The alkaline phosphatase activity of osteoblasts cultured with different concentrations of

4   PGFs was investigated. During the osteogenic differentiation, the ALP activity of MC3T3-E1 cells

5   on culture plate reached the maximum after 14 days and then decreased by day 21. In contrast, the

6   ALP activity continuously increased during the culture period with both 0.5 and 1 mg/ml of PGF.

7   Moreover, compared with the control group, the MC3T3-E1 cells cultured with PGFs exhibited

8   lower ALP activity at day 3 and day 7, but higher ALP activity at day 14 and day 21. In addition,

9   ALP activity of cells on 1 mg/ml of PGFs was significantly higher than for cells on 0.5 mg/ml of

10   PGFs at 14 and 21 days (Figure 4A). These results suggested that PGFs could promote osteoblast

11   osteogenesis and delay the differentiation process by a concentration-dependent manner.

12   To confirm the effect of PGFs on osteogenic differentiation, alizarin red staining was

13   performed to detect the possible mineral deposits on cell surfaces during osteogenic induction

14   after 0, 3, 7, 14 and 21 days (Figure 4B). The scanning images showed that more mineral

15   deposition was observed on the cells cultured with 0.5 mg/ml and 1 mg/ml of PGF and no mineral

16   formed in PGFs without cells (Figure S1). These data indicate that the PGFs could promote the

17   osteogenic differentiation of MC3T3-E1 cells.

18   **3.5 mRNA expression of osteogenic differentiation markers**

19   In order to evaluate the effect of PGFs on osteoblast differentiation during osteogenesis, the

20   mRNA expression level of osteogenesis-related marker genes including ALP, Osteocalcin (OCN),

21   Osterix (Sp7), and Collagen type I alpha 1 (Col1α1) were selected for Real-time PCR study.

22   MC3T3-E1 cells were cultured in osteogenic induction medium for 3, 7, 14 and 21 days.

23   Compared with MC3T3-E1 cells on culture plate (0 mg/ml of PGF), all of these mRNAs were

24   upregulated after 21 days of osteogenic induction on PGFs, and exhibited higher expression with

25   increasing concentration of PGFs (Figure 5). At the induction of day 3 and day 7, the expression

26   of early stage genes ALP and Sp7 in the PGF group was lower compared to the control group,

27   such delayed expression may have been due to the increased proliferation of cells on PGFs at the

28   beginning of osteogenesis.

29   **3.6 Wnt/β-catenin/Runx2 pathway analysis**

30   In order to further investigate the effects of PGFs on osteoblast differentiation, downstream

genes of Wnt signaling pathway including β-catenin and Runt-related transcription factor 2 (Runx2) were also detected by Real-time PCR assay. Runx2, which is regulated by β-catenin in Wnt signaling pathway, is an important transcription factor for osteoclast generation. Two target genes of β-catenin, Axin2 and c-myc, were regarded as positive control. The results showed that PGFs upregulated β-catenin after 7 days of induction. The expression of Runx2, Axin2 and c-myc were also significantly upregulated in the PGF group at 21 days (Figure 6A).

MC3T3-E1 cells were cultured on PGFs in osteogenic induction medium for 21 days and the impact of PGFs on the protein expression of Runx2 was then examined by immunofluorescence assay. The results showed that the protein expression of Runx2 was upregulated in the cells cultured with PGFs (Figure 6B). Thus, we suggest that PGFs could promote osteogenic differentiation by upregulating Runx2 expression through Wnt/β-catenin signal pathway.

4. Discussion

As a bioactive material for bone tissue engineering, phosphate glass fibers (PGFs) have been found to be biocompatible and osteo-conductive to bone-related cells, such as osteoblasts and bone marrow derived MSCs[11, 32]. The P50 PGFs possess the ability of releasing calcium ions in a sustained released manner, which would be highly beneficial for cell attachment and differentiation[12, 19]. In addition, the present study demonstrated that P50 PGFs of ~10 μm diameter with interlaced oriented topography significantly increased osteoblast adhesion, spreading, proliferation and differentiation during osteogenesis. The most important factor observed was that the PGFs investigated promoted osteogenic differentiation, indicated by the up-regulated expression of osteogenic marker genes, increased ALP activity and extracellular matrix mineralization, as suggested through Wnt/β-catenin signal pathway by regulating transcription factor Runx2. Therefore, for the development of synthetic orthopaedic devices based on PGFs, the design of fiber orientation and the release of therapeutic ions would be very highly beneficial.

It is well known that the topography of biomaterials can have significant influence on regulating cell behavior such as cell attachment, spreading and proliferation[33-35]. Yiping Li et al. reported that increased cell spreading area of randomly oriented fibrous scaffolds promoted the spreading of MSCs with more filopodia[36]. As demonstrated in this study, osteoblasts cultured on the interlaced PGF meshes were more inclined to spread among the PGFs with increasing concentrations. Compared with cells on culture plate with orientated cellular actin filaments and

1 fibroblast-like shape, F-actin of MC3T3-E1 cells on PGFs showed wide spreading of cellular actin

2 filaments with polygonal cell shape (Figure 2). The cytoskeletal F-actin arrangement can also

3 further influence osteoblast differentiation and function[37]. Focal adhesions emerged as diverse

4 protein complexes that provide a dynamic link of the intracellular actin cytoskeletons to an

5 extracellular matrix (ECM)[38]. Vinculin indicates the locations of focal adhesions[39]. Compared to

6 the control group, osteoblasts spread well on PGFs and the cytoskeleton displayed a better shape

7 that allowed the cells to be more prone to adhere on PGF surfaces tightly through higher expressed

8 vinculin (Figure 3A). Furthermore, the mRNA expression of adhesion-related genes including

9 Vinculin and Fibronectin 1 was increased significantly in PGF groups (Figure 3B). These

10 experimental results demonstrate that topography of PGFs could be optimized to improve cell

11 adhesion and spreading with more filopodia in the early osteogenesis stage. Furthermore, due to

12 the increased aspect ratio in the presence of PGFs, MC3T3-E1 cells cultured with PGFs

13 proliferated at a significantly faster rate than those cultured on pure culture plate alone at the early

14 stage of osteogenesis (Figure 3C). The PGFs investigated not only enhanced the initial adhesion,

15 but also promoted the proliferation of osteoblasts, indicating that these PGFs displayed superior

16 biocompatibility by providing a stable surface for a more suitable interface for the growth of

17 osteoblasts *in vitro*.

18   Apart from the surface topography of substrates, the effect of surface properties is also an

19 important factor that contributes to osteogenic response[40]. Calcium ion release has been reported

20 to be able to accelerate osteoblast differentiation with increased secretion of bone-associated

21 components *in vitro* and to enhance osseointegration *in vivo*[41-44]. In our study, the EDX analysis

22 combined with calcium ion release assay confirmed the presence of calcium within the PGFs

23 investigated and the Ca ion release profile for this P50 formulation (Figure 1B, C). Furthermore,

24 osteoblasts cultured with the P50 PGFs showed significantly increased ALP activity at 21 days of

25 osteogenic induction (Figure 4A) and the extracellular matrix mineralization assay result also

26 showed similar trends (Figure 4B). In osteogenesis, ALP activity is an important early marker and

27 mineralized nodules are a later marker for cells undergoing differentiation into mature

28 osteoblasts[20]. In addition, differentiation is also verified by assessing the induction of specific

29 genes[45]. Osteoblastic markers ALP, Col I, Sp7 and OCN were also up-regulated in cells cultured

30 with PGFs, and revealed more obvious changes in the later differentiation (Figure 5). Therefore,

calcium ion release probably acts as a major factor that contributed to osteogenic differentiation from the PGFs. It was also noticed that mRNA expression and activity of ALP of osteoblasts in PGF groups both decreased after days 3 and 7 of induction compared to the control. This inhibition effect of cell differentiation in the presence of PGFs could possibly be related to the proliferation tendency of MC3T3-E1 cells in the early stage, due to the reciprocal relationship between cell proliferation and differentiation[19, 46]. In our ongoing research, we also focus on the function of PGFs with different constituents and topography on osteoblast behavior.

It has been reported that calcium ion induced Wnt signaling is essential for bone tissue formation[25-27]. Previous studies have shown that Wnt/β-catenin/Runx2 axis stimulates osteoblast activation and subsequently leads to bone formation[47, 48]. As a main regulator, Runx2 can regulate the expression of downstream key genes, such as Col I, ALP, and OCN at the early stage of osteoblastic differentiation and the later key transcription factor Osterix[49, 50]. In the present study, real-time PCR determined that the level of β-catenin and Runx2 were significantly increased in the PGF groups (Figure 6). Immunofluorescence staining of Runx2 protein also showed greater expression in PGF groups compared to that of the control. Our results demonstrated that the mechanism of P50 PGFs on promoting osteogenesis is related to the fact that Wnt/β-catenin/Runx2 signaling pathway participates in osteogenic differentiation of osteoblasts. These results provided thus useful insight and suggest great potential of P50 PGFs for application in bone tissue engineering.

5. Conclusions

This study investigated P50 PGFs and the osteogenic mechanism that result from the interaction of osteoblasts with difference concentrations of interlaced oriented PGFs. The results demonstrated that topographical structure and bioactive ion release of P50 PGFs influence the upregulation of osteogenic marker genes, ALP activity and extracellular matrix mineralization. The P50 PGFs investigated promoted osteogenic differentiation of osteoblasts by regulating Runx2 through Wnt/β-catenin signaling pathway. Taken together, the results indicate that P50 PGFs have promising potential for application in bone tissue regeneration and biomedical device development.

Disclosures

Acknowledgement

References:

1. Jilka RL, O'Brien CA. The Role of Osteocytes in Age-Related Bone Loss. CURR OSTEOPOROS REP. 2016;14:16-25.

2. Chen X, Fan H, Deng X, et al. Scaffold Structural Microenvironmental Cues to Guide Tissue Regeneration in Bone Tissue Applications. Nanomaterials (Basel). 2018;8.

3. Wang Y, Jiang XL, Yang SC, et al. MicroRNAs in the regulation of interfacial behaviors of MSCs cultured on microgrooved surface pattern. BIOMATERIALS. 2011;32:9207-9217.

4. Huang J, Grater SV, Corbellini F, et al. Impact of order and disorder in RGD nanopatterns on cell adhesion. NANO LETT. 2009;9:1111-1116.

5. Yim EK, Darling EM, Kulangara K, et al. Nanotopography-induced changes in focal adhesions, cytoskeletal organization, and mechanical properties of human mesenchymal stem cells. BIOMATERIALS. 2010;31:1299-1306.

6. Mishra R, Bishop T, Valerio IL, et al. The potential impact of bone tissue engineering in the clinic. REGEN MED. 2016;11:571-587.

7. Hao Z, Song Z, Huang J, et al. The scaffold microenvironment for stem cell based bone tissue engineering. Biomater Sci. 2017;5:1382-1392.

8. Li J, Baker BA, Mou X, et al. Biopolymer/Calcium phosphate scaffolds for bone tissue engineering. ADV HEALTHC MATER. 2014;3:469-484.

9. He Y, Chen Q, Liu H, et al. Friction and Wear of MoO3/Graphene Oxide Modified Glass Fiber Reinforced Epoxy Nanocomposites. MACROMOL MATER ENG. 2019;304.

10. Xu J, Li K, Deng H, et al. Preparation of MCA-SiO2 and Its Flame Retardant Effects on Glass Fiber Reinforced Polypropylene. FIBER POLYM. 2019;20:120-128.

11. Ma H, Feng C, Chang J, et al. 3D-printed bioceramic scaffolds: From bone tissue engineering to tumor therapy. ACTA BIOMATER. 2018;79:37-59.

12. Ahmed I, Collins CA, Lewis MP, et al. Processing, characterisation and biocompatibility of iron-phosphate glass fibres for tissue engineering. BIOMATERIALS. 2004;25:3223-3232.

13. Mohammadi MS, Ahmed I, Muja N, et al. Effect of Si and Fe doping on calcium phosphate glass fibre reinforced polycaprolactone bone analogous composites. ACTA BIOMATER. 2012;8:1616-1626.

14. Vitale-Brovarone C, Novajra G, Lousteau J, et al. Phosphate glass fibres and their role in neuronal polarization and axonal growth direction. ACTA BIOMATER. 2012;8:1125-1136.

15. Joo NY, Knowles JC, Lee GS, et al. Effects of phosphate glass fiber-collagen scaffolds on functional recovery of completely transected rat spinal cords. ACTA BIOMATER. 2012;8:1802-1812.

16. Kim YP, Lee GS, Kim JW, et al. Phosphate glass fibres promote neurite outgrowth and early regeneration in a peripheral nerve injury model. J Tissue Eng Regen Med. 2015;9:236-246.

17. Zheng K, Wu Z, Wei J, et al. Preparation and characterization of fibrous chitosan-glued phosphate glass fiber scaffolds for bone regeneration. J Mater Sci Mater Med. 2015;26:224.

18. Alshomer F, Chaves C, Serra T, et al. Micropatterning of nanocomposite polymer scaffolds using sacrificial phosphate glass fibers for tendon tissue engineering applications. NANOMEDICINE-UK. 2017;13:1267-1277.

19. Chen Q, Jing J, Qi H, et al. Electric Field-Assisted Orientation of Short Phosphate Glass Fibers on Stainless Steel for Biomedical Applications. ACS Appl Mater Interfaces. 2018;10:11529-11538.

20. Frith J, Genever P. Transcriptional control of mesenchymal stem cell differentiation. Transfus Med Hemother. 2008;35:216-227.

21. Li Z, Xu Z, Duan C, et al. Role of TCF/LEF Transcription Factors in Bone Development and Osteogenesis. INT J MED SCI. 2018;15:1415-1422.

22. Banerjee C, Javed A, Choi JY, et al. Differential regulation of the two principal Runx2/Cbfa1 n-terminal isoforms in response to bone morphogenetic protein-2 during development of the osteoblast phenotype. ENDOCRINOLOGY. 2001;142:4026-4039.

23. Komori T. Regulation of osteoblast differentiation by transcription factors. J CELL BIOCHEM. 2006;99:1233-1239.

24. Zheng H, Guo Z, Ma Q, et al. Cbfa1/osf2 transduced bone marrow stromal cells facilitate bone formation in vitro and in vivo. Calcif Tissue Int. 2004;74:194-203.

25. Bolander J, Chai YC, Geris L, et al. Early BMP, Wnt and Ca(2+)/PKC pathway activation predicts the bone forming capacity of periosteal cells in combination with calcium phosphates. BIOMATERIALS. 2016;86:106-118.

26. Eyckmans J, Roberts SJ, Schrooten J, et al. A clinically relevant model of osteoinduction: a process requiring calcium phosphate and BMP/Wnt signalling. J CELL MOL MED. 2010;14:1845-1856.

27. Wang Y, Pan J, Zhang Y, et al. Wnt and Notch signaling pathways in calcium phosphate-enhanced osteogenic differentiation: A pilot study. J Biomed Mater Res B Appl Biomater. 2019;107:149-160.

28. Baron R, Kneissel M. WNT signaling in bone homeostasis and disease: from human mutations to treatments. NAT MED. 2013;19:179-192.

29. Lerner UH, Ohlsson C. The WNT system: background and its role in bone. J INTERN MED. 2015;277:630-649.

30. van Bezooijen RL, Ten DP, Papapoulos SE, et al. SOST/sclerostin, an osteocyte-derived negative regulator of bone formation. Cytokine Growth Factor Rev. 2005;16:319-327.

31. Felfel RM, Ahmed I, Parsons AJ, et al. In vitro degradation, flexural, compressive and shear properties of fully bioresorbable composite rods. J Mech Behav Biomed Mater. 2011;4:1462-1472.

32. Baino F, Hamzehlou S, Kargozar S. Bioactive Glasses: Where Are We and Where Are We Going? J Funct Biomater. 2018;9.

33. Huang S, Ingber DE. Shape-dependent control of cell growth, differentiation, and apoptosis: switching between attractors in cell regulatory networks. EXP CELL RES. 2000;261:91-103.

34. Wang T, Wan Y, Liu Z. Synergistic effects of bioactive ions and micro/nano-topography on the attachment, proliferation and differentiation of murine osteoblasts (MC3T3). J Mater Sci Mater Med. 2016;27:133.

35. Aminuddin NI, Ahmad R, Akbar SA, et al. Osteoblast and stem cell response to nanoscale topographies: a review. Sci Technol Adv Mater. 2016;17:698-714.

36. Li Y, Dai X, Bai Y, et al. Electroactive BaTiO3 nanoparticle-functionalized fibrous scaffolds enhance osteogenic differentiation of mesenchymal stem cells. Int J Nanomedicine. 2017;12:4007-4018.

37. Jhala D, Rather H, Vasita R. Polycaprolactone-chitosan nanofibers influence cell morphology to induce early osteogenic differentiation. Biomater Sci. 2016;4:1584-1595.

38. Katoh K. Activation of Rho-kinase and focal adhesion kinase regulates the organization of stress

fibers and focal adhesions in the central part of fibroblasts. PEERJ. 2017;5:e4063.

39. Huang J, Grater SV, Corbellini F, et al. Impact of order and disorder in RGD nanopatterns on cell adhesion. NANO LETT. 2009;9:1111-1116.

40. Viti F, Landini M, Mezzelani A, et al. Osteogenic Differentiation of MSC through Calcium Signaling Activation: Transcriptomics and Functional Analysis. PLOS ONE. 2016;11:e148173.

41. Jung GY, Park YJ, Han JS. Effects of HA released calcium ion on osteoblast differentiation. J Mater Sci Mater Med. 2010;21:1649-1654.

42. Nayab SN, Jones FH, Olsen I. Effects of calcium ion-implantation of titanium on bone cell function in vitro. J BIOMED MATER RES A. 2007;83:296-302.

43. Cheng M, Qiao Y, Wang Q, et al. Calcium Plasma Implanted Titanium Surface with Hierarchical Microstructure for Improving the Bone Formation. ACS Appl Mater Interfaces. 2015;7:13053-13061.

44. Nayab SN, Jones FH, Olsen I. Modulation of the human bone cell cycle by calcium ion-implantation of titanium. BIOMATERIALS. 2007;28:38-44.

45. Blair HC, Larrouture QC, Li Y, et al. Osteoblast Differentiation and Bone Matrix Formation In Vivo and In Vitro. Tissue Eng Part B Rev. 2017;23:268-280.

46. Bethel M, Srour EF, Kacena MA. Hematopoietic cell regulation of osteoblast proliferation and differentiation. CURR OSTEOPOROS REP. 2011;9:96-102.

47. Karner CM, Long F. Wnt signaling and cellular metabolism in osteoblasts. CELL MOL LIFE SCI. 2017;74:1649-1657.

48. Bruderer M, Richards RG, Alini M, et al. Role and regulation of RUNX2 in osteogenesis. Eur Cell Mater. 2014;28:269-286.

49. Datta HK, Ng WF, Walker JA, et al. The cell biology of bone metabolism. J CLIN PATHOL. 2008;61:577-587.

50. Komori T. Regulation of osteoblast differentiation by Runx2. ADV EXP MED BIOL. 2010;658:43-49.

1   **Figure Legends**

2   **Figure 1.** (A) SEM micrographs of PGFs. (B) the corresponding EDAX spectrum of PGFs. (C)

3   the concentration of released calcium ion from PGFs in PBS (pH=7.4) for 3 h, 6 h, 12 h, 24 h, 3 d,
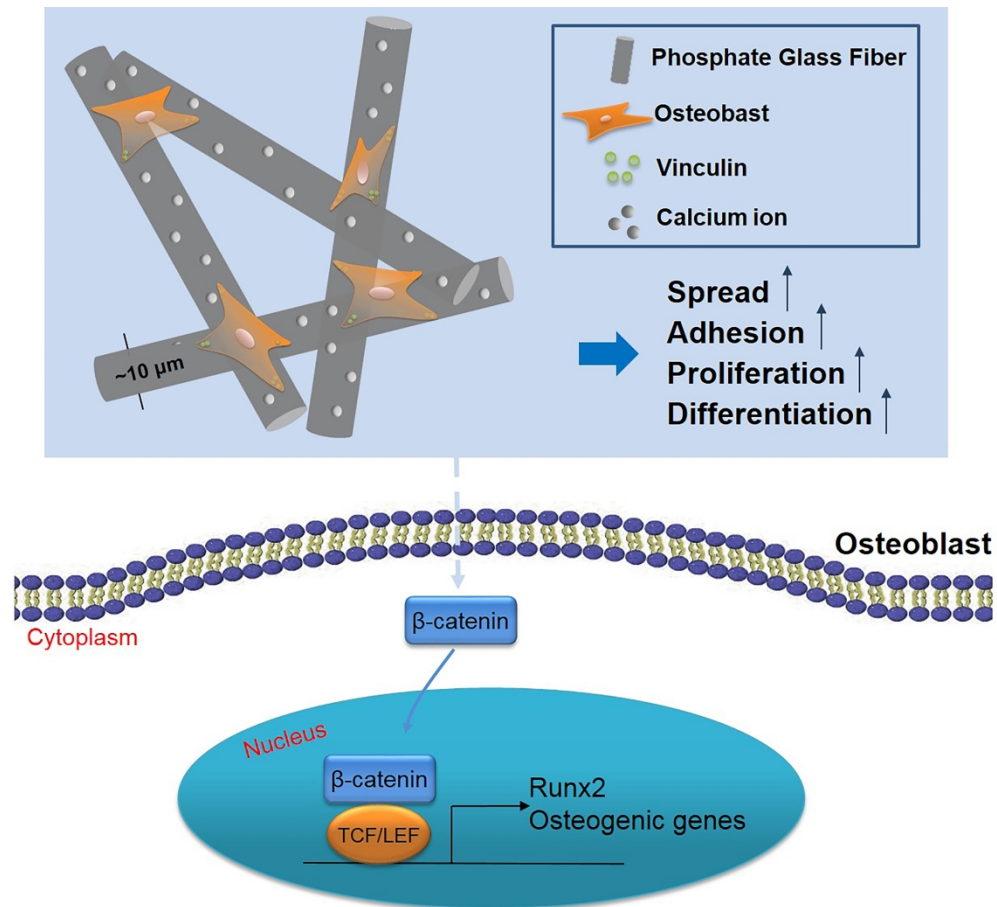
4   7 d, 14 d and 21 d.

5   **Figure 2.** (A) the morphology of MC3T3-E1 cells cultured with different concentrations of

6   interlaced oriented PGFs for 0 d, 3 d and 5 d, respectively. Scale bar: 100 μm. (B) F-actin staining

7   of cells with different concentrations of PGFs for 5 d in condition medium. Scale bar: 50 μm. The

8   arrows indicated the cells with multidirectional outspread.

9   **Figure 3.** (A) the staining of focal adhesion protein vinculin in MC3T3-E1 cells cultured with

10   different concentrations of PGFs for 3 days of induction. The arrows indicated the MC3T3-E1

11   cells with better adhesion on and among the substrates. Scale bar: 50 μm. (B) MC3T3-E1 cells

12   cultured with different concentrations of PGFs for 3 d, the expression of adhesion-related genes

13   including Vinculin, Fibronectin 1 and Collagen type Ⅲ alpha 1 (Col3α1) were measured by

14   Real-time PCR. (C) the proliferation of MC3T3-E1 cells cultured with different concentrations of

15   PGFs for 0 d, 3 d and 5 d were measured by CCK-8 assay. Data are presented as the average $\pm$

16   SD. $*p<0.05$ and $**p<0.01$ versus control group.

17   **Figure 4.** (A) ALP activity of MC3T3-E1 cells cultured with different concentrations of PGFs for

18   3 d, 7 d, 14 d and 21 d in condition medium respectively. (B) Alizarin red staining of MC3T3-E1

19   cells with different concentrations of PGF for 0 d, 3 d, 7 d, 14 d and 21 d, respectively. Data are

20   presented as the average $\pm$ SD. $*p<0.05$ and $**p<0.01$ versus control group.

21   **Figure 5.** (A-D) MC3T3-E1 cells cultured with different concentrations of PGFs for 3 d, 7 d, 14 d

22   and 21 d, respectively. The expression of osteogenic-related genes including ALP (A), OCN (B),

23   Sp7 (C), and Col1α1 (D) were measured by Real-time PCR. Data are presented as the average $\pm$

24   SD. $*p<0.05$ and $**p<0.01$ versus control group.

25   **Figure 6.** (A) MC3T3-E1 cells cultured with different concentrations of PGFs for 3 d, 7 d, 14 d

26   and 21 d, respectively. The expression of β-catenin and downstream genes Runx2, Axin2 and

27   c-myc were measured by Real-time PCR. (B) Immunofluorescence assay of Runx2 protein

28   expression was measured in MC3T3-E1 cells with different concentrations of PGFs for 21 d in

29   condition medium. Scale bar: 50 μm. Data are presented as the average $\pm$ SD. $*p<0.05$ and

30   $**p<0.01$ versus control group.

Graphical abstract: Illustration of the synergistic effects of topographical structure and released calcium ion of interlaced PGF scaffolds on osteoblast behaviors.
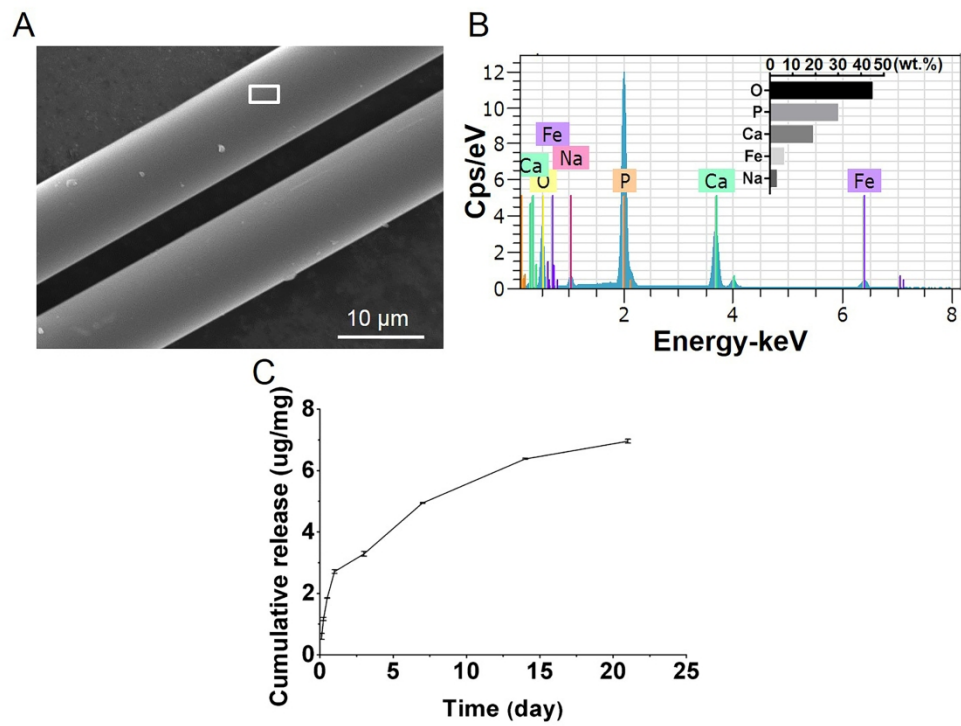
208x189mm (300 x 300 DPI)

Figure 1. (A) SEM micrographs of PGFs. (B) the corresponding EDAX spectrum of PGFs. (C) the concentration of released calcium ion from PGFs in PBS (pH=7.4) for 3 h, 6 h, 12 h, 24 h, 3 d, 7 d, 14 d and 21 d.
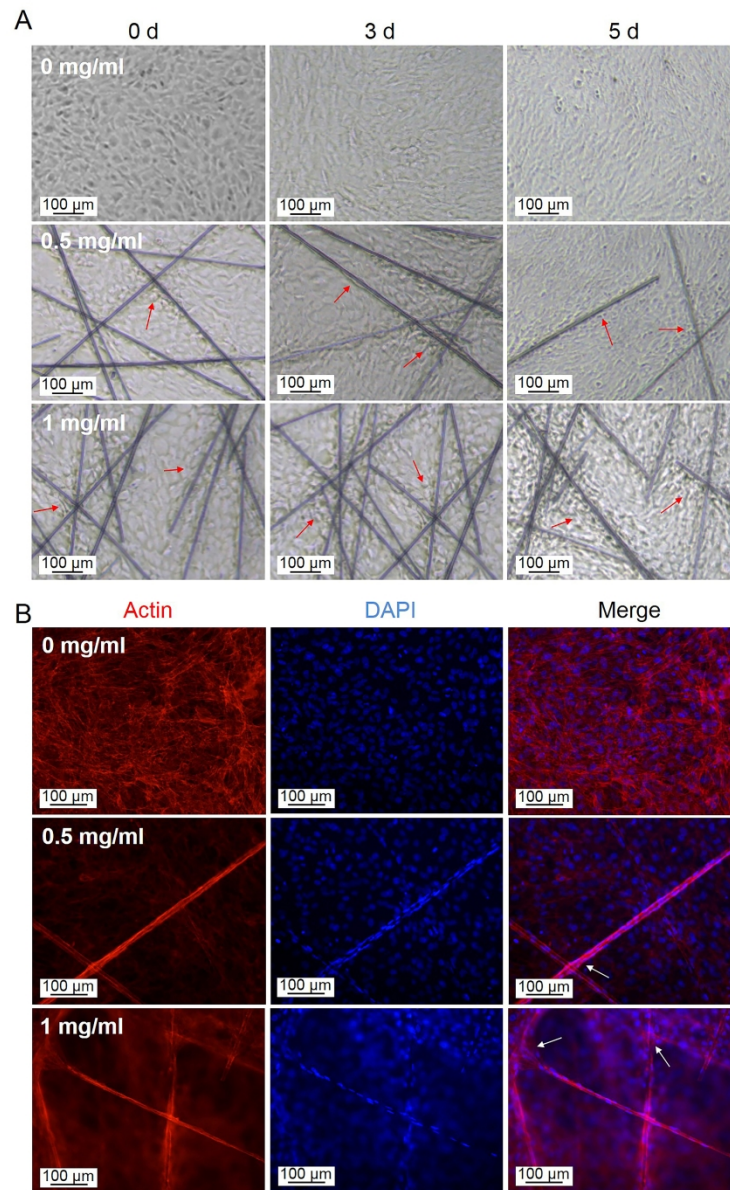
250x197mm (300 x 300 DPI)

Figure 2. (A) the morphology of MC3T3-E1 cells cultured with different concentrations of interlaced oriented PGFs for 0 d, 3 d and 5 d, respectively. Scale bar: 100 μm. (B) F-actin staining of cells with different concentrations of PGFs for 5 d in condition medium. Scale bar: 50 μm. The arrows indicated the cells with multidirectional outspread.
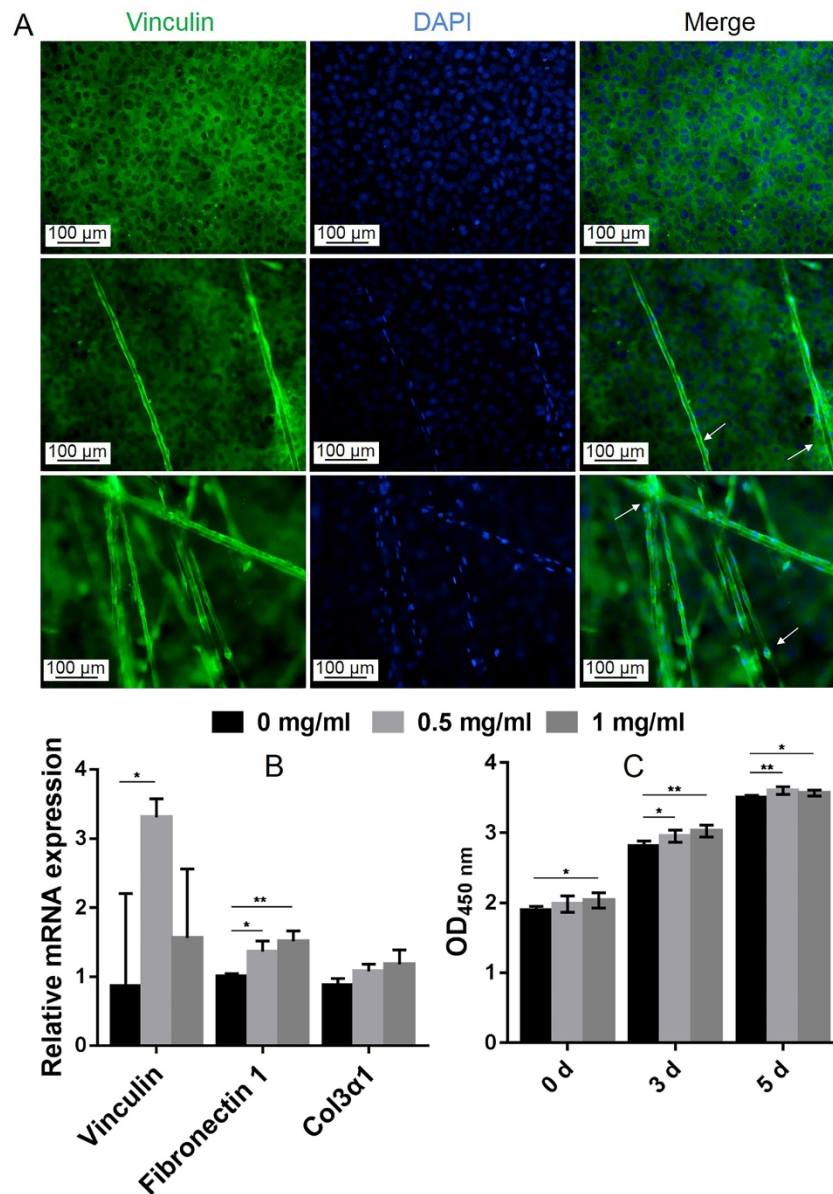
Figure 3. (A) the staining of focal adhesion protein vinculin in MC3T3-E1 cells cultured with different concentrations of PGFs for 3 days of induction. The arrows indicated the MC3T3-E1 cells with better adhesion on and among the substrates. Scale bar: 50 μm. (B) MC3T3-E1 cells cultured with different concentrations of PGFs for 3 d, the expression of adhesion-related genes including Vinculin, Fibronectin 1 and Collagen type Ⅲ alpha 1 (Col3α1) were measured by Real-time PCR. (C) the proliferation of MC3T3-E1 cells cultured with different concentrations of PGFs for 0 d, 3 d and 5 d were measured by CCK-8 assay. Data are presented as the average ± SD. *$p<0.05$ and **$p<0.01$ versus control group.
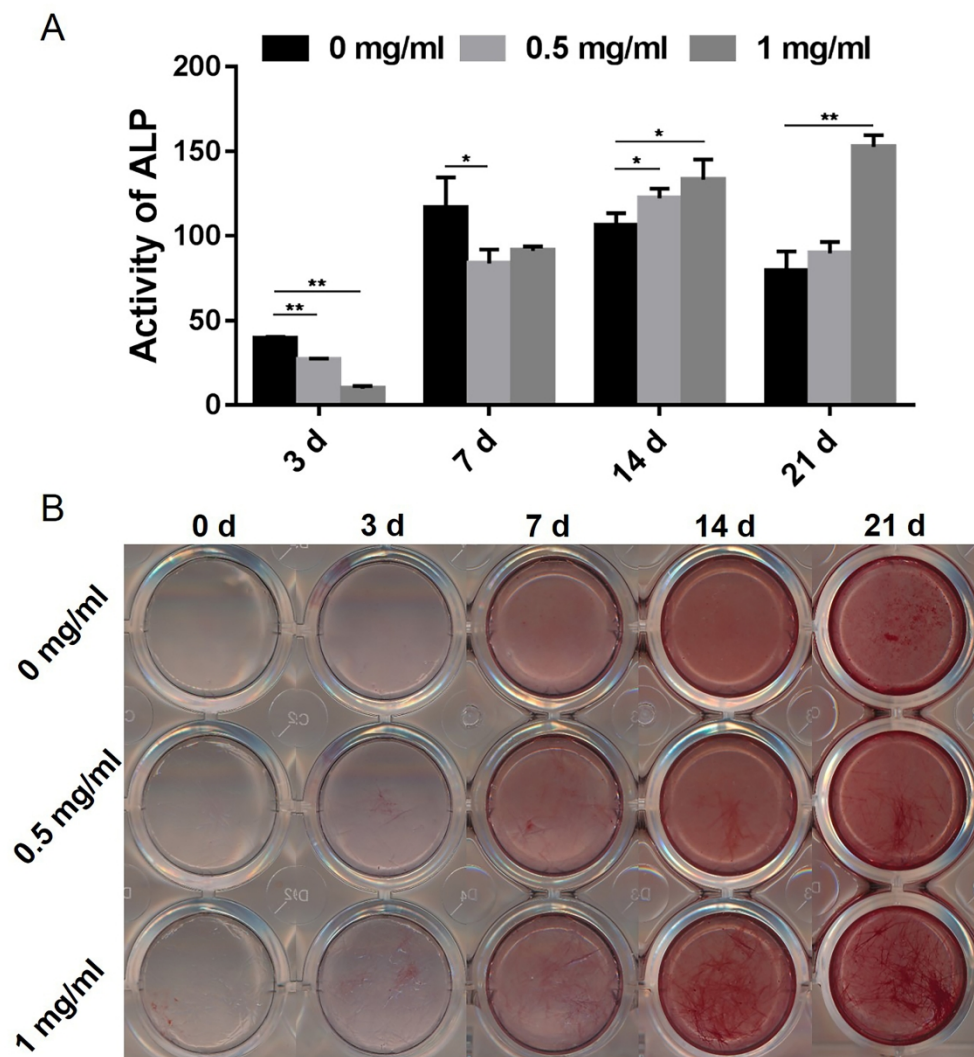
Figure 4. (A) ALP activity of MC3T3-E1 cells cultured with different concentrations of PGFs for 3 d, 7 d, 14 d and 21 d in condition medium respectively. (B) Alizarin red staining of MC3T3-E1 cells with different concentrations of PGF for 0 d, 3 d, 7 d, 14 d and 21 d, respectively. Data are presented as the average ± SD. *p<0.05 and **p<0.01 versus control group.
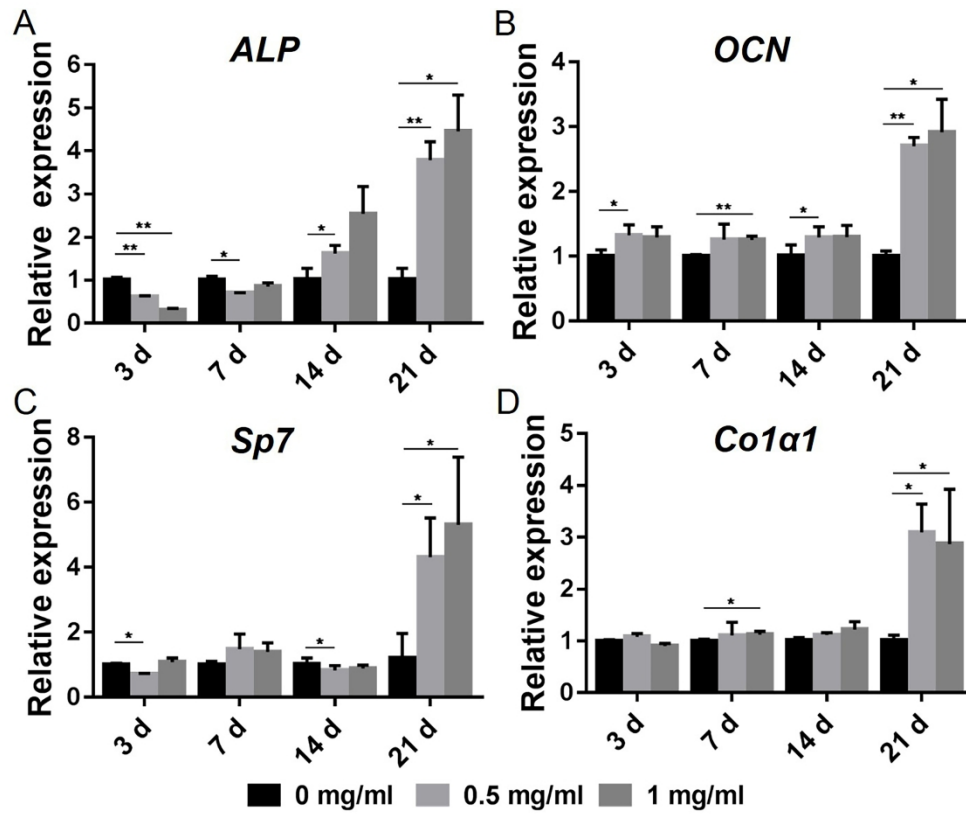
227x249mm (300 x 300 DPI)

Figure 5. (A-D) MC3T3-E1 cells cultured with different concentrations of PGFs for 3 d, 7 d, 14 d and 21 d, respectively. The expression of osteogenic-related genes including ALP (A), OCN (B), Sp7 (C), and Col1α1 (D) were measured by Real-time PCR. Data are presented as the average ± SD. *$p < 0.05$ and **$p < 0.01$ versus control group.
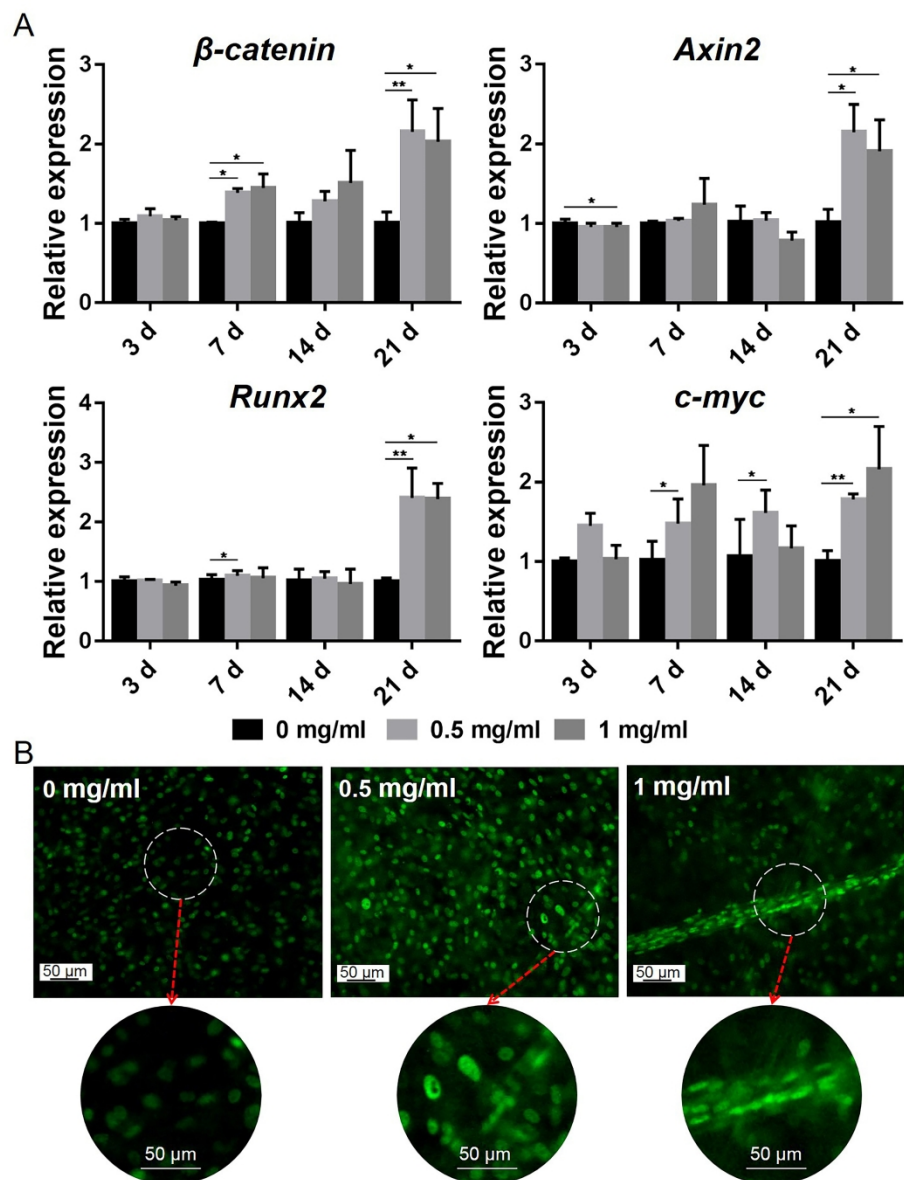
244x205mm (300 x 300 DPI)

Figure 6. (A) MC3T3-E1 cells cultured with different concentrations of PGFs for 3 d, 7 d, 14 d and 21 d, respectively. The expression of β-catenin and downstream genes Runx2, Axin2 and c-myc were measured by Real-time PCR. (B) Immunofluorescence assay of Runx2 protein expression was measured in MC3T3-E1 cells with different concentrations of PGFs for 21 d in condition medium. Scale bar: 50 μm. Data are presented as the average ± SD. *$p < 0.05$ and **$p < 0.01$ versus control group.

Table 1. Primer sequences used in Real-Time RT-PCR

Genes	Forward primer (5'-3')	Reverse primer (5'-3')
GAPDH	TGCACCACCAACTGCTTAG	GGATGCAGGGATGATGTTC
ALP	GTTGCCAAGCTGGGAAGAACAC	CCCACCCCGCTATTCCAAAC
OCN	GAACAGACTCCGGCGCTA	AGGGAGGATCAAGTCCCG
Col1α1	GAAGGCAACAGTCGATTCACC	GACTGTCTTGCCCCAAGTTCC
Sp7	TGAGCTGGAACGTCACGTGC	AAGAGGAGGCCAGCCAGACA
Runx2	CGCCCCTCCCTGAACTCT	TGCCTGCCTGGGATCTGTA
β-catenin	GGTCCTCTGTGAACTTGC	GTAATCCTGTGGCTTGTCC
Axin2	ACCTCAAGTGCAAACTCTCACCCA	AGCTGTTTCCGTGGATCTCACACT
c-myc	AGCGACTCTGAAGAAGAACA	ACATGGCACCTCTTGAGGAC
Vinculin	GATGCTGGTGAACTCAATGA	CGAATGATCTCGTTAATCTC
Fibronectin 1	GCGACTCTGACTGGCCTTAC	CCGTGTAAGGGTCAAAGCAT
Col3α1	GTCCACGAGGTGACAAAGGT	CATCTTTTCCAGGAGGTCCA